Nanoscale

Programmed assembly of polymer–DNA conjugate nanoparticles with optical readout and sequence-specific activation of biorecognition†

Johannes P. Magnusson,[a] Francisco Fernández-Trillo,[b] Giovanna Sicilia,[a] Sebastian G. Spain*[a] and Cameron Alexander*[a]

Soft micellar nanoparticles can be prepared from DNA conjugates designed to assemble via base pairing such that strands containing a polymer corona and a cholesterol tail generate controlled supramolecular architecture. Functionalization of one DNA conjugate strand with a biorecognition ligand results in shielding of the ligand when in the micelle, while encoding of the DNA sequences with overhangs allows supramolecular unpacking by addition of a complementary strand and sequence-specific unshielding of the ligand. The molecular assembly/disassembly and 'on–off' switch of the recognition signal is visualized by FRET pair signalling, PAGE and a facile turbidimetric binding assay, allowing direct and amplified readout of nucleic acid sequence recognition.

Introduction

The encoding of information into materials through monomer sequence is a central process in nature, utilising components with Ångstrom-scale dimensions to build devices that operate over nanometre and micron lengthscales. Natural materials of this type are essentially 'soft' nanomachines, with structures that are flexible enough to assemble, dissociate and recombine rapidly, enabling functions such as replication, transcription and translation. Nucleic acid components of this cellular machinery have evolved primarily as biological information storage and transfer materials, but increasingly their potential as synthetic operators and actuators is being realized as chemists exploit new DNA and RNA sequences for functions not previously seen in nature.[1–3] These include molecular computers,[4] motors,[5] nanoreactors,[6] as well as carriers, sensors and diagnostics.[7–12] In addition, the ability to encode 'dormant' information in DNA sequences, i.e. structures generated from paired nucleic acids that are stable until exposed to a complementary sequence, enables DNA assemblies to be used for logic operations important in a biomedical context.[13,14]

A common obstacle in translating a drug candidate from in vitro efficacy to clinical applicability is ensuring that the active compound reaches the disease site while minimising off-target effects. For most anti-cancer drugs this is particularly

problematic as they are often hydrophobic, leading to indiscriminate diffusion into tissue when administered systemically (intravenously). Combined with the inherent cytotoxicity of these drugs this leads to severe side effects that limit the administrable dose and thus clinical efficacy. Encapsulation of a drug within nanoparticles reduces its ability to permeate into tissues resulting in increased circulation times. Additionally, the enhanced permeation and retention (EPR) effect,[15,16] where macromolecules and nanoparticles migrate across the 'leaky' vasculature of tumour sites and are retained there, allows for passive targeting of tumours. A more advanced class of delivery vehicles are those which that respond to an additional stimulus so that, once accumulated at the tumour site, they may be activated to either release the drug or promote cellular uptake. For example, Salmaso et al. demonstrated that gold nanoparticles coated with a temperature-responsive polymer and non-temperature responsive polymer bearing folate were only taken up by folate-receptor positive cells when the responsive segments were collapsed.[17] A similar deshielding approach has recently been demonstrated by Mirkin et al.[18] These examples used temperature as a stimulus, however temperature is a 'crude' stimulus and difficult to control in vivo, thus replacement of the responsive elements with nucleic acid assemblies should allow for greater specificity. Many elegant studies have reported the use of DNA-assemblies and logic operators on solid nanoparticle supports, such as gold, silver, metal oxides and quantum dots.[19–21] While highly effective in diagnostic applications, 'hard' nanoparticles of this type are less attractive from the viewpoint of combined signalling and therapeutic delivery applications, as the solid core limits their loading with bioactive molecules as well as reducing the inherent flexibility of the nanoparticle framework. Furthermore, recent reports have

[a]School of Pharmacy, University of Nottingham, University Park, Nottingham, NG7 2RD, UK. E-mail: sebastian.spain@nottingham.ac.uk; cameron.alexander@nottingham.ac.uk; Fax: +44 (0)115 951 5122; Tel: +44 (0)115 846 6272

[b]School of Chemistry, University of Birmingham, Edgbaston, Birmingham, B15 2TT, UK
† Electronic supplementary information (ESI) available: Full experimental procedures and additional supporting figures. See DOI: 10.1039/c3nr04952c
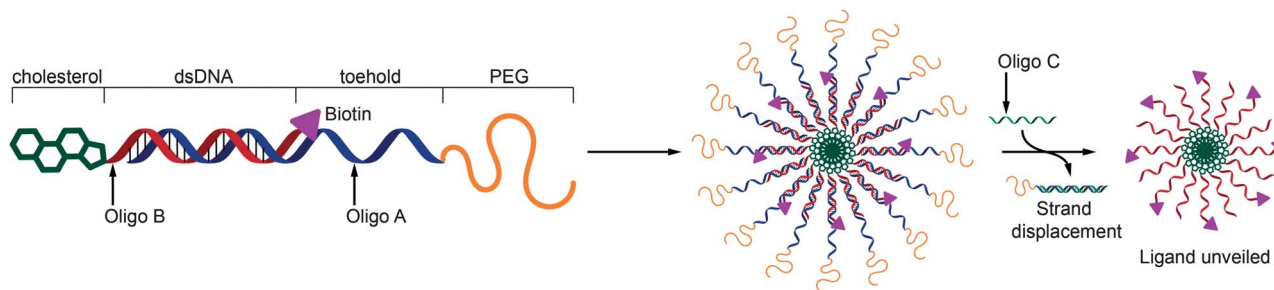
Fig. 1 Schematic representation of the structure of DNA conjugates and the unshielding of a ligand *via* strand displacement. Oligo A holds a PEG chain to provide shielding, oligo B is complementary to part of oligo A and is modified with cholesterol and biotin. When annealed the resulting hybrid forms a micellar structure with the ligand shielded. Oligo C is a DNA sequence complementary to oligo A resulting in strand displacement and unshielding of the ligand (biotin).

indicated that some metal-based nanoparticles can induce pro-inflammatory and pro-apoptotic effects.[22–24] Accordingly there are advantages in the biomedical field for nanoparticles based solely on organic components.

Here we aim to demonstrate that 'soft', and serum-stable micellar nanoparticles with a nucleic acid reporter function can be self-assembled from polymer–DNA conjugates. The design motif utilises a strand-matching architecture to project a shielding polymer corona that hides a biological recognition signal (biotin). The system was designed to include toehold sequences in the nucleic acid segments such that the micelles may be selectively unshielded by addition of a competing complementary strand resulting in presentation of the signal for binding (Fig. 1).

Experimental section

Materials

Oligonucleotides (HPLC purified) except strand A2 were purchased from biomers.net GmbH (Ulm, Germany) and were used without purification. Strand A2 (HPLC purified) was purchased from Sigma-Aldrich and used without further purification. For sequences and modifications see Table 1. Poly(ethylene glycol) monomethyl ether (M_n 1900 Da) was purchased from Polysciences Europe GmbH (Eppelheim, Germany). N,N'-Disuccinimidyl carbonate (95%), tris-borate-EDTA buffer (TBE, 10× concentrate), acrylamide/bis-acrylamide 29/1 (40% solution), ammonium persulfate (≥98%), N,N,N',N'-tetramethylethylenediamine (TEMED, 99%), orange G, formamide (>95.5%, BioReagent), ethylenediaminetetraacetic acid disodium salt (EDTA, >99%), urea (electrophoresis grade), tris(hydroxymethyl)aminomethane hydrochloride (tris·HCl, >99%), acetic acid (>99%), triethylamine (TEA, >99%), glycerol (>98%), 3-hydroxypicolinic acid (3-HPA), diammonium hydrogen citrate (DAHC), water (BPC grade), Stains-All (95%), methylene blue hydrate (>97%), fetal bovine serum (FBS), avidin (BioUltra, 10–15 units per mg protein) and sodium phosphotungstate tribasic hydrate (puriss. p.a.) were purchased from Sigma-Aldrich (Gillingham, UK). Dulbecco's phosphate-buffered saline (DPBS, without Ca^{2+} and Mg^{2+}) was purchased from Lonza. Anhydrous DMSO (>99.5%, <50 ppm water) was

purchased from Acros. All other solvents were Fisher HPLC or analytical grade and used without further purification.

Synthesis of α-methoxy-ω-succinimidyl carbonate poly-[ethylene glycol]1900 (mPEG-NHS)

Poly[ethylene glycol] monomethyl ether (M_n 1900 g mol^{-1}, 1.9 g, 1 mmol) was dried by azeotropic distillation with toluene and then dissolved in dichloromethane/triethylamine/acetonitrile (4 mL, 2.5/0.5/1). N,N'-Disuccinimidyl carbonate (640 mg, 2.5 mmol) was added and the reaction mixture stirred at room temperature overnight (16 h). The resulting solution was precipitated with diethyl ether/petrol and the resulting solid isolated by centrifugation. The product was purified by dissolution in DCM and reprecipitation in diethyl ether/petrol for two further times.

^{1}H NMR (400 MHz, chloroform-d) δ = 4.54–4.39 (m, 2H, CH_2 adjacent to carbonate), 3.92–3.44 (m, PEG backbone), 3.39 (s, 3H, MeO–), 2.85 (s, 4H, succinimidyl CH_2). NMR analysis was consistent with >95% conversion of the terminal hydroxyl to the succinimidyl carbonate.

Synthesis of PEG-A1

Oligo A1 (10 mg, 1.42 μmol) was resuspended in 2 mL of Dulbecco's PBS (DPBS) at pH 7.5. mPEG-NHS (14.5 mg, 7.1 μmol) was dissolved in 200 μL of DMSO and added dropwise to the oligonucleotide solution. The conjugation was allowed to proceed for 24 hours. After 24 hours the coupling efficiency was examined using high performance liquid chromatography (HPLC, see below for details). HPLC analysis revealed that only around 50% of the starting oligonucleotide had coupled to the PEG in 24 hours, another 2.5 equivalents of mPEG-NHS (7.25 mg, 3.55 μmol) in 100 μL of DMSO were therefore added to the reaction and it was allowed to proceed for a further 24 hours. The reaction was again monitored by HPLC after 48 hours, HPLC analysis showed 66% conversion. Another 5 equivalents of mPEG-NHS (14.5 mg, 7.1 μmol) in 200 μL of DMSO were added to the reaction and left to react for a further 24 hours. Analysis after 72 hours revealed that conjugation had achieved roughly 80% coupling efficiency. At this time point the reaction was stopped and lyophilized. The crude mixture was resuspended in DNase free water (1 mL) and purified by

semi-preparative HPLC (see conditions below). The volume collected was concentrated under reduced pressure (to remove organic solvent) and then subsequently lyophilized to remove the water. PEG-A1 was collected as a white powder, the powder was dissolved in DNase free water and quantified using optical density at 260 nm. In total, 251 OD (7.5 mg, 75% yield) of PEG-A1 were recovered as the pure product. The product was aliquoted into vials, freeze dried and then kept at −20 °C prior to being used. The pure product was analysed by MALDI-TOF. Mass expected: 8965 g mol^{-1}. Mass found: 9320 g mol^{-1}.

Synthesis of PEG-A3

Oligo A3 (0.5 mg, 0.066 μmol) was resuspended in 188 μL of Dulbecco PBS (DPBS) at pH 7.5. mPEG-NHS (0.67 mg, 0.328 μmol) was dissolved in 60 μL of DMSO and added dropwise to the oligonucleotide solution. The conjugation was allowed to proceed for 24 hours. After 24 hours the coupling efficiency was examined using HPLC (see below for details). HPLC analysis revealed that only around 6% of the starting oligonucleotide had coupled to the PEG in 24 hours, consequently another 5 equivalents of mPEG-NHS (1.34 mg, 0.656 μmol) in 100 μL of DMSO were added to the reaction and it was allowed to proceed for a further 24 hours. The reaction was again monitored by HPLC after 48 hours, HPLC analysis showed 44% conversion. Another 2.5 equivalents of mPEG-NHS (0.67 mg, 0.328 μmol) in 100 μL of DMSO along with 100 μL of THF were added to the reaction and left to react for another 96 hours. Analysis after 144 hours revealed that conjugation had achieved roughly 80% coupling efficiency. At this time the reaction was stopped, the organic solvent was removed under reduced pressure and the water removed using lyophilization. The crude mixture was afterwards resuspended in DNase free water (1 mL) and purified by semi-preparative HPLC (see conditions below). The solution collected was concentrated under reduced pressure (to remove organic solvent) and then subsequently lyophilized to remove the water. PEG-A3 was collected as a purple powder, which was dissolved in DNase free water and quantified using optical density at 260 nm. PEG-A3 (6.3 OD, 180 μg, 36% yield) was recovered as a pure product. This conjugate was aliquoted into vials, freeze dried and then kept at −20 °C prior to being used. The identity of the product was determined by MALDI-TOF. Mass expected: 9520 g mol^{-1}. Mass found: 9840 g mol^{-1}.

HPLC analysis and purification of DNA strands

Reverse phase high performance liquid chromatography (RP-HPLC) was performed on a Shimadzu Prominence UPLC system fitted with a DGU-20A5 degasser, LC-20AD low-pressure gradient pump, CBM-20A LITE system controller, SIL-20A autosampler and an SPD-M20A diode array detector. Analytical separations were performed on a Phenomenex Clarity 3 μm Oligo-RP C18 column (4.6 × 50 mm) with a gradient of MeOH (10–70% for PEG-A1 and 35–70% for PEG-A3 over 20 min) in 0.1 M triethylammonium acetate (TEAA, pH 7.5)/MeCN (95/5) at a flow rate of 1.0 mL min^{-1} as a mobile phase. Semi-preparative

separations were performed on a Phenomenex Clarity 3 μm Oligo-RP C18 column (10 × 50 mm) under the same conditions at a flow rate of 5.0 mL min^{-1}.

MALDI analysis

Matrix-assisted laser desorption/ionization time-of-flight (MALDI-TOF) mass spectrometry was performed on a Bruker MALDI-TOF Ultraflex III spectrometer operated in linear, positive ion mode. 3-HPA containing DAHC was used as the matrix for the oligonucleotide analysis. Briefly, a saturated solution of 3-HPA (50 mg mL^{-1}) was prepared by adding 25 mg of 3-HPA to 500 μL of 50% ACN/water. 25 μL of DAHC solution (100 mg mL^{-1}) was added to 225 μL of the 3-HPA solution, to give a final DAHC concentration of 10 mg mL^{-1}. Equal volumes of matrix solution and ODN solution (0.2 mM) were mixed and 2 μL of the mixture was spotted onto the MALDI plate and allowed to dry.

Polyacrylamide gel electrophoresis (PAGE)

Denaturing PAGE

Preparation of samples. Samples were prepared by dilution in denaturing loading buffer and heating to 95 °C for 2 minutes before rapid cooling ice.

Preparation of gels. Gel casting solution was prepared by mixing the components described in Table S2† and carefully pipetted into preassembled plate. A 10-well comb was inserted and the gel allowed to set for 45 min.

Electrophoresis. Gels were pre-run for 20 min at 200 V in 1× TBE. Wells were then washed with the same buffer and samples loaded at approximately 200 pmoles per well. Gels were run at 200 V until the Orange G loading dye had migrated off the bottom of the gel (approximately 80 min).

Staining. Gels were washed with water then stained with 0.02% methylene blue in 1× TBE for 20 minutes. Excess stain was removed by destaining with distilled water until the bands were clear against the background. Images were recorded using a standard flat bed scanner (HP Scanjet 2710).

Native PAGE

Preparation of samples. Samples were prepared by dilution in native loading buffer. Loading dye (Orange G) was added only to the ladder.

Preparation of gels. Gel casting solution was prepared by mixing the components described in Table S2† and carefully pipetted into preassembled plate. A 10-well comb was inserted and the gel allowed to set for 45 min.

Electrophoresis. Gels were pre-run for 20 min at 200 V in 1× TBE. Wells were washed with the same buffer and samples loaded at approximately 200 pmoles per well. Gels were run at 200 V until the Orange G loading dye was approximately 1 cm from the bottom of the gel (approximately 80 min).

Staining. Gels were washed with water then stained with Stains-All staining solution for 20 minutes in the dark. Staining solution was removed and gels destained until bands were clearly visible against background. Gels were imaged as before.

Hybridization of DNA strands

Strands to be hybridized were mixed in equimolar quantities at a concentration of 50–150 μM in hybridization buffer and placed in a 95 °C water bath. The water bath was allowed to cool to room temperature over a period of 2 hours.

Dynamic light-scattering (DLS)

Dynamic light-scattering was performed using a Viscotek 802 DLS instrument fitted with an internal laser (λ 830 ± 5 nm, Pmax 60 mW). Hybrid PEG-A1:B1 (50 μM in annealing buffer) was filtered through a 0.45 μm membrane (Whatman Spartan, regenerated cellulose) prior to analysis. Laser power was adjusted to until detection rate of at least 300 kcps was achieved. A series of 10 × 3 seconds experiments was recorded and hydrodynamic radii distributions calculated with Viscotek/Malvern OmniSize3 software.

Transmission electron microscopy

Transmission electron microscopy (TEM) was performed on an FEI Tecnai 12 Biotwin microscope. Samples were prepared by first treating a holey carbon-coated 400 mesh copper TEM grid with graphene oxide solution (0.1 mg mL^{-1}) for 30 min. Excess graphene oxide solution was wicked away with the aid of filter paper and the grids dried for 30 min. Oligonucleotide solution (10 μL, 5 μM) was then placed on the grid; after 2 minutes the excess liquid was wicked away with the aid of filter paper and the sample allowed to dry for 5 min. Samples were stained by addition of 5 μL of a 3% solution of sodium phosphotungstate for 1 min before wicking away as before. Samples were then dried overnight prior to imaging.

Stability assay

Hybrid PEG-A1:B1 (50 μM) or A2:C in DPBS were mixed with FBS at a ratio of 9/1 and incubated at 37 °C. Aliquots were removed at 0, 24, 48 and 72 h. and frozen until later analysis. Samples were analyzed by native PAGE as described previously.

Strand displacement assays

By PAGE. The hybrid to be analyzed was combined with either complementary (strand C) or scrambled (strand D) DNA at equimolar quantities in hybridization buffer at a final concentration of 10 μM for both hybrid and displacement strand. Samples were incubated at room temperature for 1 h and then analysed by native PAGE as described previously.

By FRET/fluorimetry. Fluorescence experiments were performed using a Varian Cary Eclipse spectrophotometer (λ_{ex} 494 nm, excitation slit width 2.5 mm; λ_{em} 519 nm, emission slit width 5 mm). Hybrids PEG-A1:B1 and PEG-A3:B3 were combined at a 4/1 mole ratio in hybridization buffer at a total concentration of 5 μM (*i.e.* 1 μM fluorophore). 500 μL aliquots were added to a fluorescence cuvette and the fluorescence measured over a period of 10 minutes. After this time 25 μL of 100 μM (1 mole equiv.) of oligonucleotide C or D, or an equivalent volume of buffer, was added to the cuvette and the fluorescence measured for a further

30 min. Emission intensities were baseline corrected to the emission intensity at $t = 0$ min.

Percentage emission was calculated using background fluorescence prior to strand addition as zero and the fluorescence of a solution containing 1 μM strand B3 as 100%. Full emission spectra were recorded prior to addition of DNA and 30 min post addition.

Avidin–biotin binding assay

Avidin was dissolved in DPBS at a concentration of 0.2 mg mL^{-1} protein (2.5 units per mL) and aliquots (100 μL) were transferred to the wells of a 96-well plate. 25 μL of PEG-A1:B2 (50 μM) was added to each well followed by 75 μL of oligo C (100 μM, 6 mol equiv.), oligo D (100 μM, 6 mol equiv.), or buffer alone. Additional control wells were prepared by combining avidin (100 μL), buffer (25 μL) and oligo C (75 μL). Samples were incubated for 30 min before the absorbance at 550 nm was measured using a plate reader (Tecan Infinite M200).

Results and discussion

Design, synthesis and analysis of polymer–DNA conjugates

The use of nanoparticles in diagnosis and therapy requires the solving of numerous synthetic and biological challenges. Systems of this type may need to encapsulate a drug or a signal molecule, traverse complex biological barriers and then report a disease event or release a drug at a determined time point and/or a specific cellular or external cue. A 'soft' nanoparticle structure is advantageous in this environment because biological membranes are inherently flexible and a number of studies have shown that micelle- and vesicle-like nanoparticles exhibit better biodistribution and cell uptake properties than more rigid analogues.[25–27] In addition, a more fluid-like structure at a nanoparticle surface facilitates macromolecular exchange interactions, such as ligand–receptor interactions or nucleic acid strand switching. A particularly important example of a switching operation in the drug delivery context is the need to keep a recognition ligand on a polymer or particle hidden/dormant but to expose the specific functionality in response to a biological trigger. Viruses carry out operations of this type to sequentially expose cell entry ligands and endosomal escape functionality, and this 'hide-reveal' concept has been used in synthetic viral-mimetic polymers[28,29] and thermo-responsive nanoparticles[17,30] to enhance drug delivery and selective cell entry.

Accordingly, we set out a design concept for 'hide-reveal' nanoparticles, utilizing DNA-strand recognition to encode for sequence specific assembly and derivitisation at the respective 3′ and 5′ ends of each to direct functionality to the interior and exterior of the particle as shown schematically in Fig. 1. The oligonucleotide sequences and the modifications required (a) to assemble the structures, (b) to incorporate an orthogonal biological recognition signal (biotin), (c) to provide a shielding polymer at the exterior (PEG), and (d) to unveil the ligand *via* competitive strand displacement are given in Table 1.

The primary chain of Oligo A is 22 bases long and 5′-modified with a poly(ethylene glycol) chain to provide

Table 1 Sequences and modifications of oligonucleotides used

Name	5′	Sequence	3′
A1	Amino	TAACAGGATTAGCAGAGCGAGG	—
PEG-A1	PEG	TAACAGGATTAGCAGAGCGAGG	—
A2	—	TAACAGGATTAGCAGAGCGAGG	—
A3	Amino	TAACAGGATTAGCAGAGCGAGG	BHQ-1[a]
PEG-A3	PEG	TAACAGGATTAGCAGAGCGAGG	BHQ-1[a]
B1	Cholesterol	CCTCGCTCTGCT	—
B2	Cholesterol	CCTCGCTCTGCT	Biotin
B3	Cholesterol	CCTCGCTCTGCT	Fluorescein
C	—	CCTCGCTCTGCTAATCCTGTTA	—
D	—	AGGAGAGTAGCGAGCTAGTCAA	—

[a] Black Hole Quencher 1 (Biosearch Technologies).

protection and shielding. Oligo B is 5′-modified with cholesterol and the 3′-terminus of Oligo B is modified with a biotin moiety. Oligo B is complementary to the 12 bases at the 3′ terminus of oligo A allowing hybridization via Watson–Crick base-pairing to yield a hybrid that shields the biotin moiety within the micelle. The 10 base toehold allows disruption of the hybrid upon addition of Oligo C which is complementary to the full 22 bases of Oligo A. Displacement of Oligo A results in unshielding of the micelle exposing the biotin moieties and making them accessible to bind avidin.

PEGylation of amino-modified oligos A1 and A3 was achieved by reaction with succinimidyl carbonate-activated PEG (Scheme S1†) followed by purification by high pressure liquid chromatography (HPLC). Successful conjugation was confirmed by PAGE, HPLC and MALDI-TOF mass spectrometry (Fig. 2A, S2 and S3† respectively). Subsequent assembly of the conjugates into supramolecular structures was achieved by a simple mixing/ annealing process. Hybridization of strand PEG-A1 with strand cholesterol oligo B1 to produce hybrid PEG-A1:B1 led to the formation of discrete objects, as apparent in dynamic light-scattering (DLS, Fig. 2C and S4†) and transmission electron microscopy (TEM). The DLS intensity distribution (Fig. 2C, black line) is dominated by a population centered at $R_h \sim 100$ nm with small populations at 26 and 2 nm. The number distribution (Fig. 2C, red line), calculated from intensity distribution in the range $2 < R_h < 10^3$ nm, shows a main population with R_h 25 nm and small population at 60 nm. This agrees well with TEM where objects approximately 40 nm diameter are observed although dispersity is higher (Fig. 2D). In addition, labeled hybrids could be formed by hybridization of PEG-A1 with chol-biotin oligo B2 (hybrid PEG-A1:B2), and PEG-A3 (3′-quencher) with chol-fluorescein oligo B3 (hybrid PEG-A3:B3, labeled for FRET).

If DNA conjugates are to be used in vitro/vivo then they need to be stable under physiological conditions. Consequently, the stability of micellar hybrid PEG-A1:B1 towards degradation by serum enzymes (including nucleases) was determined by incubation with 10% fetal calf serum (FCS) at 37 °C and analysis by native PAGE. Hybrid PEG-A1:B1 was considerably more stable to degradation compared to unmodified (i.e. no 3′ or 5′ modifications) hybrid A2:C (Fig. S6†) with little evident degradation over 72 h; however, the band-broadening imparted by the PEGylation makes quantitative analysis difficult. The

comparative stability is expected as "spherical nucleic acids"[11] have been previously demonstrated to be more stable than the linear form[31] and the additional PEG coating should further reduce the accessibility of the DNA segments to nucleases.

Strand displacement and unshielding of micelles

The "programmable" responsive unshielding was investigated by PAGE and FRET analysis. For PAGE experiments, hybrids were incubated with 1 molar equivalent of either oligonucleotide C (complementary) or D (scrambled) at room temperature. Samples were then analyzed by native PAGE (Fig. 3A and S7†). When incubated with complementary oligo C (Lane 7) the band for hybrid PEG-A1:B1 is lost (cf. Lane 4) and bands for chol oligo B1 and hybrid PEG-A1:C found in its place (cf. Lanes 3 and 6 respectively). Conversely, when incubated with scrambled oligo D the PEG-A1:B1 band still remains and no new bands are observed.‡ Equivalent bands were observed for the hybrids PEG-A1:B2 and PEG-A3:B3 when analysed in the same manner (Fig. S7A and B†).

For FRET experiments hybrids PEG-A1:B1 and PEG-A3:B3 were mixed at a 4/1 ratio. PEG-A3:B3 has a fluorescein and a quencher moiety (Black Hole Quencher 1, BHQ-1, Biosearch Technologies) attached to the 3′ ends of the strands forming the duplex. While the duplex is intact, FRET from the fluorescein to BHQ-1 results in minimal fluorescence and an 'off' state. If the double helix is disrupted FRET is lost resulting in switching 'on' of the fluorescence (Fig. 3B). Samples were incubated for 10 min to determine a baseline then 1 equivalent of complementary oligo C or scrambled oligo D, or an equivalent volume of buffer, was added and emission monitored for a further 30 minutes. Addition of either oligo D or buffer alone results in a minimal decrease in emission intensity due to a small dilution of the solution. As expected, addition of oligo C results in a rapid increase in emission before the fluorescence reached a plateau value. These data agree with that from the PAGE experiments and confirm that the micelle corona may be removed by addition of a complementary DNA strand.

Comparison of these data to those for an equivalent concentration of the chol-fluorescein oligo B3 alone confirms restoration of approximately 45% of the expected fluorescence (Fig. S8B†). Although this is lower than expected it likely results from incomplete unshielding due to steric hindrance resulting in some quencher remaining in close enough proximity to the fluorescein to maintain FRET.

Finally, to determine if unpacking could be used for the presentation of the targeting ligand for binding, micelles of hybrid PEG-A1:B2 were evaluated in a biotin–avidin binding assay. Briefly, PEG-A1:B2 was mixed with avidin in the presence of oligo C, oligo D or buffer alone. If unpacking is successful the biotin will bind to the avidin resulting in crosslinking, and subsequent precipitation, that may be quantified by measuring the solution turbidity (absorbance at 550 nm, Fig. 3D). Turbidity

---

‡ It should be noted that in lanes 8 and 9 in Fig. 3A and S6 there is an extra band observed with a molecular weight between that of oligo D and hybrid PEG-A1:B1. As it also appears in the lane where only oligo D was added we conclude that this is due to self-assembly of oligo D.
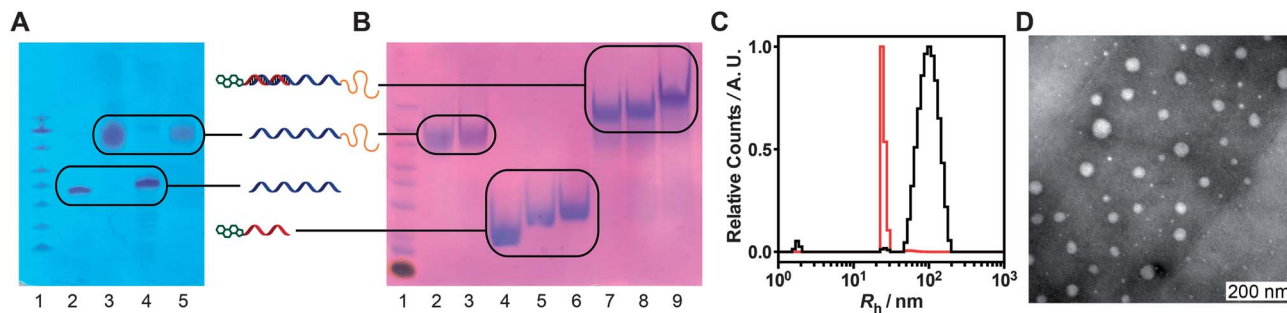
Fig. 2 (A) Denaturing PAGE of oligonucleotides before and after PEGylation. Lanes: 1. Ladder, 2. A1, 3. PEG-A1, 4. A3, 5. PEG-A3. (B) Native PAGE of oligonucleotides and hybrids. Lanes: 1. Ladder, 2. PEG-A1, 3. PEG-A3, 4. B1, 5. B2, 6. B3, 7. hybrid PEG-A1:B1, 8. hybrid PEG-A1:B2, 9. hybrid PEG-A3:B3. (C) Dynamic light-scattering of hybrid PEG-A1:B1. Intensity distribution (black line) and number distribution (red line). (D) Transmission electron micrograph of hybrid PEG-A1:B1 stained with sodium phosphotungstate.
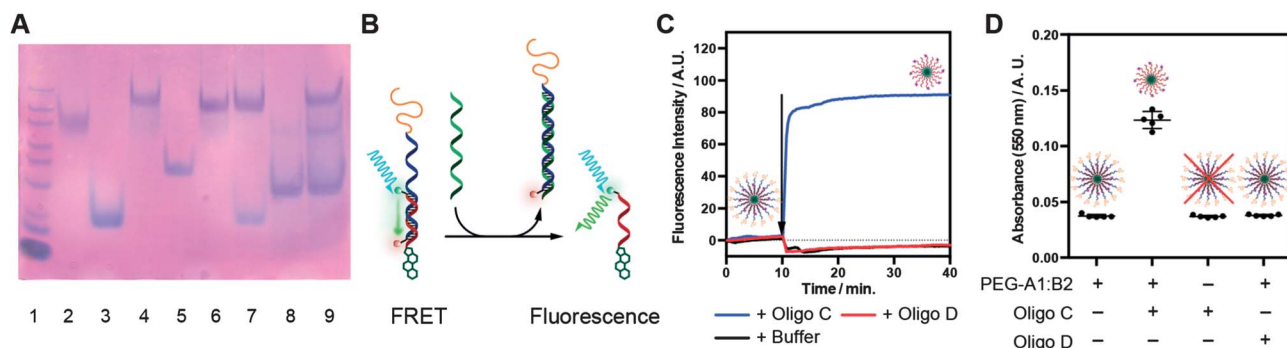

Fig. 3 (A) Strand displacement analyzed by PAGE. Lanes: (1) Ladder, (2) PEG-A1, (3) B1, (4) PEG-A1:B1, (5) C, (6) PEG-A1:C, (7) PEG-A1:B1 + C, (8) D, (9) PEG-A1:B1 + D. (B) Schematic of specific oligonucleotide detection *via* disruption of Förster Resonance Energy Transfer (FRET). When complementary oligonucleotide is added hybrid PEG-A3:B3 is disrupted resulting in loss of FRET and a consequential increase in fluorescence. (C) Baseline corrected fluorescence intensity of mixed micelles of PEG-A1:B1 and PEG-A3:B3 (4/1 mole ratio) before and after addition of complementary oligo C (blue), scrambled oligo D (red), or an equivalent volume of buffer (black). (D) Turbidimetry measurements (absorbance at 550 nm) of avidin solutions treated with combinations of PEG-A1:B2, complementary oligo C and scrambled oligo D. Circles represent individual measurements, lines represent mean and bars represent standard deviation. There is only a detectable increase in absorbance when both PEG-A1:B2 and oligo C are present.

measurements demonstrate addition of complementary oligo C results in a significant increase in absorbance compared to the avidin treated with PEG-A1:B2 alone ($p < 0.0001$, 1-way ANOVA); addition of scrambled oligo D had no effect on absorbance confirming sequence specific binding. Additionally, to confirm that turbidity was caused by unpacking and not a sequence specific interaction between oligo C and avidin, the same measurement was performed in the absence of PEG-A1:B2 and no effect on turbidity was observed.

Conclusions

In conclusion we have demonstrated that oligonucleotide sequences may be used to direct the supramolecular assembly and unshielding of micellar nanoparticles in a pre-programmable manner. The DNA conjugate micelles formed rapidly and displayed high stability to serum enzymes as well as securely shielding a recognition ligand in the absence of a specific nucleic acid strand. Unveiling of the ligand by addition of the complementary strand was easily detected by a simple turbidimetry assay

in which the protein, avidin, bound to the exposed biotin signals. Experiments to evaluate the ability of DNA conjugates to switch in response to specific sequences *in vitro* and *in vivo* are continuing in our laboratories.[32] Programmable control over ligand presentation may have important applications in drug-delivery, *e.g.* controlled targeting in the presence of a therapeutic nucleic acid sequence. In addition, sensing applications can be envisioned for systems that, like the FRET pair shown herein, can modulate their spectral properties in a programmable way allowing for *in vitro* and *in vivo* monitoring of unshielding. Finally, the flexibility in the design and synthesis offered by nucleic acid based materials combined with the opportunity to tailor polymers and ligands for specific biomedical tasks suggests materials of this type may prove useful in the personalized diagnostics and patient-group stratified therapeutics.

Acknowledgements

Notes and references

1 J. Zheng, J. J. Birktoft, Y. Chen, T. Wang, R. Sha, P. E. Constantinou, S. L. Ginell, C. Mao and N. C. Seeman, *Nature*, 2009, **461**, 74–77.

2 D. Y. Zhang, A. J. Turberfield, B. Yurke and E. Winfree, *Science*, 2007, **318**, 1121–1125.

3 T. Ciengshin, R. Sha and N. C. Seeman, *Angew. Chem., Int. Ed.*, 2011, **50**, 4419–4422.

4 B. Chakraborty, N. Jonoska and N. C. Seeman, *Chem. Sci.*, 2012, **3**, 168–176.

5 J. Bath, S. J. Green and A. J. Turberfield, *Angew. Chem., Int. Ed.*, 2005, **44**, 4358–4361.

6 M. L. McKee, P. J. Milnes, J. Bath, E. Stulz, A. J. Turberfield and R. K. O'Reilly, *Angew. Chem., Int. Ed.*, 2010, **49**, 7948–7951.

7 Y. H. Roh, J. B. Lee, P. Kiatwuthinon, M. R. Hartman, J. J. Cha, S. H. Um, D. A. Muller and D. Luo, *Small*, 2011, **7**, 74–78.

8 Y. H. Roh, R. C. H. Ruiz, S. Peng, J. B. Lee and D. Luo, *Chem. Soc. Rev.*, 2011, **40**, 5730–5744.

9 M.-P. Chien, M. P. Thompson and N. C. Gianneschi, *Chem. Commun.*, 2011, **47**, 167–169.

10 M.-P. Chien, A. M. Rush, M. P. Thompson and N. C. Gianneschi, *Angew. Chem., Int. Ed.*, 2010, **49**, 5076–5080.

11 J. I. Cutler, E. Auyeung and C. A. Mirkin, *J. Am. Chem. Soc.*, 2012, **134**, 1376–1391.

12 J. I. Cutler, K. Zhang, D. Zheng, E. Auyeung, A. E. Prigodich and C. A. Mirkin, *J. Am. Chem. Soc.*, 2011, **133**, 9254–9257.

13 F. E. Alemdaroglu, N. C. Alemdaroglu, P. Langguth and A. Herrmann, *Adv. Mater.*, 2008, **20**, 899–902.

14 H. Lee, A. K. R. Lytton-Jean, Y. Chen, K. T. Love, A. I. Park, E. D. Karagiannis, A. Sehgal, W. Querbes, C. S. Zurenko, M. Jayaraman, C. G. Peng, K. Charisse, A. Borodovsky, M. Manoharan, J. S. Donahoe, J. Truelove, M. Nahrendorf, R. Langer and D. G. Anderson, *Nat. Nanotechnol.*, 2012, **7**, 389–393.

15 J. Fang, H. Nakamura and H. Maeda, *Adv. Drug Delivery Rev.*, 2011, **63**, 136–151.

16 V. Torchilin, *Adv. Drug Delivery Rev.*, 2011, **63**, 131–135.

17 F. Mastrotto, P. Caliceti, V. Amendola, S. Bersani, J. P. Magnusson, M. Meneghetti, G. Mantovani, C. Alexander and S. Salmaso, *Chem. Commun.*, 2011, **47**, 9846–9848.

18 K. Zhang, X. Zhu, F. Jia, E. Auyeung and C. A. Mirkin, *J. Am. Chem. Soc.*, 2013, **135**, 14102–14105.

19 S. S. Agasti, S. Rana, M. H. Park, C. K. Kim, C. C. You and V. M. Rotello, *Adv. Drug Delivery Rev.*, 2010, **62**, 316–328.

20 M. M. C. Cheng, G. Cuda, Y. L. Bunimovich, M. Gaspari, J. R. Heath, H. D. Hill, C. A. Mirkin, A. J. Nijdam, R. Terracciano, T. Thundat and M. Ferrari, *Curr. Opin. Chem. Biol.*, 2006, **10**, 11–19.

21 P. Zrazhevskiy, M. Sena and X. Gao, *Chem. Soc. Rev.*, 2010, **39**, 4326–4354.

22 M. Sharma, R. L. Salisbury, E. I. Maurer, S. M. Hussain and C. E. W. Sulentic, *Nanoscale*, 2013, **5**, 3747–3756.

23 D. Choudhury, P. L. Xavier, K. Chaudhari, R. John, A. K. Dasgupta, T. Pradeep and G. Chakrabarti, *Nanoscale*, 2013, **5**, 4476–4489.

24 K. Luyts, D. Napierska, B. Nemery and P. H. M. Hoet, *Environ. Sci.: Processes Impacts*, 2013, **15**, 23–38.

25 I. Canton and G. Battaglia, *Chem. Soc. Rev.*, 2012, **41**, 2718–2739.

26 J. W. Yoo, E. Chambers and S. Mitragotri, *Curr. Pharm. Des.*, 2010, **16**, 2298–2307.

27 Y. Geng, P. Dalhaimer, S. Cai, R. Tsai, M. Tewari, T. Minko and D. E. Discher, *Nat. Nanotechnol.*, 2007, **2**, 249–255.

28 M. Soliman, R. Nasanit, S. R. Abulateefeh, S. Allen, M. C. Davies, S. S. Briggs, L. W. Seymour, J. A. Preece, A. M. Grabowska, S. A. Watson and C. Alexander, *Mol. Pharmaceutics*, 2012, **9**, 1–13.

29 Y. Nie, D. Schaffert, W. Rödl, M. Ogris, E. Wagner and M. Günther, *J. Controlled Release*, 2011, **152**, 127–134.

30 S. R. Abulateefeh, S. G. Spain, K. J. Thurecht, J. W. Aylott, W. C. Chan, M. C. Garnett and C. Alexander, *Biomater. Sci.*, 2013, **1**, 434–442.

31 D. S. Seferos, A. E. Prigodich, D. A. Giljohann, P. C. Patel and C. A. Mirkin, *Nano Lett.*, 2009, **9**, 308–311.

32 G. Yasayan, J. P. Magnusson, G. Sicilia, S. G. Spain, S. Allen, M. C. Davies and C. Alexander, *Phys. Chem. Chem. Phys.*, 2013, **15**, 16263–16274.